**Article:**

Chung Kim Yuen, S., Nurick, G.N., Langdon, G.S. orcid.org/0000-0002-0396-9787 et al. (1 more author) (2017) Deformation of thin plates subjected to impulsive load : Part III – an update 25 years on. International Journal of Impact Engineering, 107. pp. 108-117. ISSN 0734-743X

https://doi.org/10.1016/j.ijimpeng.2016.06.010

# Accepted Manuscript


Title: Deformation of thin plates subjected to impulsive load: part III – an update 25 years on

Author: S. Chung Kim Yuen, G.N. Nurick, G.S. Langdon, Y. Iyer

PII: S0734-743X(16)30395-5
DOI: http://dx.doi.org/doi: 10.1016/j.ijimpeng.2016.06.010
Reference: IE 2720

To appear in: International Journal of Impact Engineering

Received date: 17-2-2016
Revised date: 15-6-2016
Accepted date: 22-6-2016

Please cite this article as: S. Chung Kim Yuen, G.N. Nurick, G.S. Langdon, Y. Iyer, Deformation of thin plates subjected to impulsive load: part III – an update 25 years on, International Journal of Impact Engineering (2016), http://dx.doi.org/doi: 10.1016/j.ijimpeng.2016.06.010.

# Deformation of Thin Plates Subjected to Impulsive Load: Part III – An Update 25 years on

S. Chung Kim Yuen, G. N. Nurick, G. S. Langdon and Y. Iyer

Blast Impact and Survivability Research Unit (BISRU), Department of Mechanical Engineering, University of Cape Town, Private Bag, Rondebosch 7701

*Corresponding author email: Genevieve.langdon@uct.ac.za

Highlights

- Air blast experiments on flat steel plates
- Review of 25 years of blast experimentation
- Update of dimensionless analysis
- Check to see that post 1989 test data correlates with dimensionless analysis approaches

**Abstract**

In 1989, Nurick and Martin published two review papers on the deformation of thin steel plates subjected to impulsive air-blast loading. The state of the art has progressed significantly in the following 25 years, and this review paper restricts itself to experimental studies that investigate the response of monolithic metal plates subjected to air-blast loading generated by detonating plastic explosive. From the large numbers of experiments reported, it is shown that the failure progressions in circular and quadrangular plates are similar and can be adequately described by three "failure modes" – namely large plastic deformation (mode I), tensile tearing (mode II) and shearing (mode III) although the severity and location of these failures on the plates is primarily determined by spatial distribution of the blast loading across the plate surface, and that boundary conditions significantly influence the onset of shearing and tearing failures due to variation in the in-plane movement of the plate material.

The non-dimensional analysis approaches used by Nurick and Martin have been expanded to include the effects of load localisation and stand-off distance, and show good correlation with the expanded sets of test data published since 1989. It is concluded that these approaches still hold merit as simple tools for evaluating the likely effect of a close proximity air blast load on a flat metal plate.

**Keywords**

Blast loading, plates, failure modes, deformation, non-dimensional analysis

## Notation

| | |
|---|---|
| B | plate width |
| I | impulse |
| L | plate length |
| R | exposed plate radius |
| $R_o$ | charge radius |
| S | stand-off distance |
| t | plate thickness |
| W | TNT equivalent mass |
| Z | Hopkinson scaled distance |
| $\delta$ | permanent mid-point displacement |
| $\phi_c$ | non-dimensional impulse for circular plates |
| $\phi_{cS}$ | non-dimensional impulse for circular plates, incorporating stand-off distance |
| $\phi_q$ | non-dimensional impulse for quadrangular plates |
| $\rho$ | material density |
| $\sigma$ | characteristic stress = quasi-static yield stress |

## 1. Introduction

The study of structural response to impulsive blast loading has been performed for many years. In 1989, Nurick and Martin[1, 2] reviewed data from previous experimental and theoretical investigations into the response of flat, monolithic metal plates subjected to blast loading. In addition, new experimental data was reported and non-dimensional analysis was utilised with the aim of developing a simple, empirical prediction of the displacement of a blast loaded plate with fully clamped boundary condition[2]. Since 1989, there have been many experimental, analytical and numerical modelling investigations into the response of structures to blast loading. These have expanded the types of structures examined to include different plate geometries, stiffened and welded structures, sandwich panels, composite materials and monolithic metal plates with different boundary conditions. Tensile tearing and shear failures have also been investigated alongside large plastic deformation responses. Different forms of loading, including localised loading and stand-off distance effects have also been studied.

This paper reviews the literature that has published since 1989 in an attempt to update the work presented by Nurick and Martin[1, 2]. Using the post 1989 developments in non-dimensional analysis, much of the more recent experimental data is then translated into non-dimensional impulse and displacement parameters and plotted alongside the data presented in ref[2] to determine if the empirical relationships proposed in 1989 are still valid.  Due to the myriad of papers in this area, this review paper restricts itself to experimental studies that investigate the response of monolithic metal plates subjected to air-blast loading generated by detonating plastic explosive. Unless otherwise stated, the reviewed results are concerned with flat mild steel plates.

## 2. Experimental studies since 1989

In order to summarise the experimental work performed in the past twenty five years, the studies presented in the literature are summarised in Table 1 according to the following classifications:

- Loading type: uniform, localised, varying stand-off distance,
- Plate geometry: circular or quadrangular; stiffened or flat,
- Boundary conditions, and
- Failure mode: large plastic deformation, tensile tearing, shear failure.

### 2.1 Uniform loading conditions

Teeling-Smith and Nurick[3] investigated the progression in failure of clamped circular plates subjected to uniform blast loading. Photographs of plate failures at different impulses are shown in Figure 1. At low impulse levels, large plastic deformation (known as Mode I failure) was observed, with mid-point displacement increasing with increasing impulse. As impulse was increased, thinning occurred at the plate boundary (known as Mode Ia or Mode Ib, depending upon the proportion of the circumference that exhibited necking) which was a precursor to tensile tearing along the boundary edge[3]. As impulse reached a threshold value, partial tearing (known as Mode II*) of the plate edge occurred. This Mode II* failure is the transition between Mode I and Mode II (tensile tearing of the boundary edge) failure. As impulse increased further, plates exhibited tensile tearing of the boundary edge. If the impulse was increased beyond the threshold required for complete boundary tearing, the mid-point displacement of the plates decreased with increasing impulse and the failure mode tended towards transverse boundary shear (known as Mode III)[3]. The observed failure modes were similar to those reported by Menkes and Opat[4] for explosively loaded beams and the definitions of the failure modes are summarised in Table 2 for blast-loaded plates.

Nurick and co-workers[5, 6] investigated the influence of boundary conditions on the failure of uniformly loaded circular plates in follow-on studies from the work reported in ref[3]. Thomas and Nurick[5] compared the fully clamped and built-in boundary conditions and showed that the boundary condition has little influence upon plate response during Mode I (large plastic deformation) failures. However, the onset of boundary thinning and subsequently boundary tearing were significantly influenced by the type of boundary condition. The built-in plates exhibited the onset of thinning and tearing at lower impulses since the boundary was more rigid and the clamped boundary was unable to fully prevent in-plane movement of the plate[5]. There was also a difference in the curvature of the plates at the boundary – the clamped plates exhibited curvature within the clamped region whereas the built-in plate curvatures began at the built-in edge[5]. Nurick et al.[6] investigated the effect of a sharp or filleted edge on the response of fully clamped circular plates. The filleted edge clamps delayed the onset of thinning and tearing failures to higher plate displacements, whereas the sharp edged clamp failed at the lowest impulse levels. The sharp edge caused an indentation in the plate which initiates necking[6]. Plates with curved edges exhibited necking without any indentations, similar to that observed during tensile test[6].

Cloete et al.[7] reported results from tests involving uniformly loaded clamped circular plates. In additional to the boundary clamping, the plates either had a centrally located hole (referred to as annular) or were prevented from deforming with a central support. The central support was a Hopkinson bar, enabling transient force measurements to be taken during the structural response phase. During the annular plate tests, the duration of the blast load was typically in the order of 50 ms and showed the classical blast wave characteristics of a sudden rise followed by an exponential decay. Three distinct modes of failure for fully clamped circular plates were observed from the tests on plates with a central support. The failure mode definitions were similar but not identical to those reported for circular plates[3]. A distinction was made between tensile and shear failures that occur prior to and subsequent to large plastic deformation, something which was only possible due to the transient measurements from the Hopkinson bar. The maximum transverse shear stress that the plates could sustain along the inner boundary was relatively consistent and marked the transition from failure subsequent to large deformation and failure prior to large deformation[7].

Olson et al.[8] and Nurick and Shave[9] investigated the progression in failure of clamped quadrangular plates subjected to uniform blast loading. Photographs of plate failures reported in ref[9] are shown in Figure 2. Similar failures modes were observed for quadrangular plates as for circular plates, when the work in refs[8, 9] is compared to the work of Teeling-Smith and Nurick[3]. At low impulse levels, large plastic deformation was again observed, with mid-point displacement increasing with increasing impulse. As impulse was increased, thinning occurred at the centre of the plate boundary which progressed to tearing failure with further increases in impulse[8, 9]. The tensile tearing also initiated at the centre of one of the boundary edges and progressed towards the corners at higher impulses[8]. In-plane movement (often referred to as “pulling-in”) was observed as displacement increased and tearing occurred[8]. If the impulse was increased beyond that required for complete boundary tearing, the mid-point displacement of the plates decreased with increasing impulse and the failure mode tended towards transverse boundary shear (known as Mode III).

Bonorchis and Nurick[10] extended the work on boundary conditions reported in refs [5, 6] to study the influence of boundary conditions on the response of quadrangular plates subjected to uniform loading. Plates with clamped, built-in and welded (both TIG and MIG) boundaries were tested under the same loading conditions. Similarly to the results obtained by Thomas and Nurick[5] for circular plates, large plastic deformation response was unaffected by boundary condition, but the initiation of tensile failure was significantly influenced by the imposed boundary condition. The impulse required for boundary tearing was lowest for the built-in plates and next lowest for the welded plates. The clamped plates required the highest impulse to initiate tearing, again due to the in-plane movement of the clamped plates.

**2.2 Localised blast loading**

Nurick and co-workers[11, 12] reported results from localised blast tests on fully clamped circular plates. The loading was generated by detonating centrally located disks of plastic explosive (PE4) in close proximity to the plates. The dimensions of the PE4 disk (diameter and charge height) were varied, along with charge mass, to produce a range of responses in the plates from low levels of plastic deformation through to tearing of the plates in the central region. Photographs of failed plates are shown in Figures 3 and 4[13]. The localisation of the loading caused a change in plate profile when compared to uniformly loaded plates. Instead of a single dome, the locally loaded plates exhibited a global dome with a secondary inner dome superimposed on top in the central region. The inner dome diameter increased with increased charge diameter, as might be expected. At higher impulses, thinning and tearing occurred in the central region, followed by capping failure. After capping, the remaining plate has a centrally located hole, the diameter of which is also proportional to the charge diameter. As impulse increased beyond that required for capping, radial cracks propagated in the plate away from the central cap and caused petalling failure.

Yuen and Nurick[13] investigated the effects of load-plate diameter ratio and plate thickness on the response of locally blast-loaded circular plates with built-in boundaries. In many tests, the same capping failures observed in refs[11, 12] were observed, but it was also shown that thicker plates with small load diameters exhibited petalling failures rather than capping failure. Once the load-plate diameter was greater than or equal to 0.4, the loading was less localised and tearing failure occurred at the plate boundary rather than in the central region.

Jacob et al.[14] reported a study on the influence of plate and load geometry on the response of clamped quadrangular plates subjected to localised blast loading. Plate thickness was varied from 1.6 mm to 4 mm. The plate aspect ratio was varied from 1:1 (square) to 2.4:1 (rectangular). Various charge diameters and charge masses were used. It was found, that over the whole range of plate thicknesses, charge diameters and aspect ratios, the response of the quadrangular plates was similar in form to that of circular plates[14]. Photographs of some typical plate profiles are shown in Figure 5, where the inner dome atop a global dome is again observed for Mode I failure (followed by capping failure at higher impulses) as it was for circular plates in refs[11-13]. Similar results were reported by Langdon et al.[15] for built-in square plates subjected to localised blast loads.



### 2.3 Plates subjected to blast loading at different stand-off distances

Jacob et al.[16] performed an experimental investigation into the influence of stand-off distance on the response of clamped circular plates. The blast loading was generated by detonating small disks of PE4 at the open end of a tube. The tube directed the blast loading towards the clamped target plate. The plate had a diameter of 106 mm and a thickness of 1.6 mm. Various tube lengths were used to provide stand-off distances ranging from 25 to 300 mm. Large plastic deformation occurred in most of the experiments. At low stand-off distances (up to 40 mm), the plate response was typical of those observed for locally loaded plates refs [11-13]. At large stand-off distances (above 100 mm), the plate response was typical of uniformly loaded plates, with stand-off distances between 40 and 100 mm, being described as a transition between the two loading regimes. Increasing stand-off distance therefore decreases load localisation. Jacob et al.[16] concluded that loading could be considered to be uniform when the stand-off distance exceeded the largest plate dimension

Neuberger et al.[17, 18] performed scaled experiments where the blast loading was generated by detonating spherical TNT charges (varying mass from 0.468 kg to 8.75 kg) at different stand-off distances (65 mm to 200 mm). The clamped circular test plates had diameters of either 0.5 m or 1 m and were manufactured from RHA steel. The main foci of the investigations were the achievement of geometrically similar scaling during the blast tests[17] and the influence of spring-back on response[18]. Neuberger et al. [17, 18] observed large plastic deformation of the plates that was similar to that observed by Jacob et al. [16].

Jacinto et al.[19] reported results from large scale experiments on quadrangular plates. The loading was generated by detonating charges with equivalent TNT masses varying from 0.8 kg to 10 kg at stand-off distances of 30 m and 60 m. Two sets of plates were tested – one with dimensions 1.5 m by 1m by 2 mm (with three free edges and one edge clamped in a concrete base) and one with dimensions 0.95 m by 0.95 m by 0.9 mm (clamped in a frame on all four sides). Due to the large stand-off distance relative to the plate size, the loading was assumed to be uniformly distributed. Pressure transducers recorded transient pressure histories that were typical of far field loading, as shown in Figure 6. Most of the paper was focussed upon numerical modelling. Jacinto et al.[19] commented that the plates clamped in frames showed greater vibrational damping than the plates with one edge clamped in a concrete base. This observation reinforces the findings reported by Nurick et al.[5, 6, 10, 20] on the importance of boundary conditions.

Large scale field tests involving the detonation of up to 26300 kg of ordnance per test were reported by Yuen et al.[21, 22]. Square plates (exposed area of 0.5 by 0.5 m) were clamped in test frames and situated at various stand-off distances from the explosive detonation site. The ordnance was laid out on the ground in carpet-like form (rather than the typical cylindrical or spherical shaped charges used in laboratories). The location of the charge on the ground, unusual explosive layout and casing of the explosive due to the ordnance types led to complex loading conditions (with ground effects, geometry effects and fragmentation damage respectively). Despite the complex loading, the resulting deformation was similar to that observed in lab-scale tests involving uniformly loaded clamped square plates[8, 9]. At the closer stand-off distances the ordnance casings became projectiles as a result of the explosions and perforated some of the plates. The perforation damage, however, seemed to have little influence on the global response of the panels. Hopkinson-Cranz scaling was used (and modified) to evaluate the loading parameters and allow empirical predictions of mid-point displacement. The empirical predictions gave reasonable agreement with the experimental results.



**2.4 Stiffened plates**

Investigations into the response of stiffened plates to blast loading have mainly focussed on uniformly distributed loading[23-35]. As might have been anticipated, the addition of stiffeners, whether they are clamped into position[29, 31], welded[32], integral with the plate[30, 33], or riveted[34, 35] resulted in lower global displacements for a given impulse.

Schleyer et al.[32] showed that the direction of loading and the amount of in-plane restraint influenced the response of stiffened plates subjected to pulse pressure loading. Loading the plates such that the stiffeners were in tension resulted in slightly increased mid-point displacement compared with loading the plates with the stiffeners in compression. Plates with no in-plane restraint exhibited displacements that were much larger than those with in-plane restraint along the boundary edges[32]. The addition of stiffeners to the unrestrained plates had no discernable effect upon displacement[32]. The geometry, number and position of the stiffeners are of importance in the response of clamped plates. Yuen and Nurick[33] showed that uniformly loaded plates with more stiffeners are more effective at reducing permanent displacements, and that locating the stiffener along the mid-lines of the plates is more effective at reducing displacements than placing stiffeners at other positions. Stiffeners were shown to reduce the plate deformations but this led to the initiation of tearing failures at lower impulses when compared to unstiffened flat plate responses[33]. Tearing initiated along the plate boundary, usually along the side parallel to the stiffeners.

Localised loading of the same stiffened plates used by Yuen and Nurick[33] was reported by Langdon et al.[15]. A general failure progression of the stiffened plates emerged from the experimental results[15]: localised central dome, limited by the stiffener geometry; thinning along the stiffener-plate edges; tearing away from the stiffener edge and towards the boundary; petalling and in one case, stiffener rupture. The locations of tearing were strongly dependent upon the stiffener location[15], as shown in the photographs in Figure 7.

## 3. Non-dimensional analysis

Non-dimensional analysis can be used to compare the results from experiments performed on panels of different scale, different material properties and tested under different loading conditions.

**3.1 Circular plates**

In 1989, Nurick and Martin[1, 2] derived an expression, shown in Eq. (1) for circular plates, that provided a non-dimensional impulse parameter for comparing blast-loaded panels of different geometries (exposed radii and thicknesses) and different materials (densities and characteristic stresses), to be treated similarly. The expression for non-dimensional impulse given in Eq. (1) was then modified by Nurick and Martin[2] for localised blast loading of circular plates as shown in Eq. (2). The experimental studies conducted since 1989 have provided additional insight into the behaviour of plates under different loading conditions and greater understanding of the factors affecting plate performance. In parallel with the experimental studies reported above, Nurick and co-workers[14, 16] have further developed the non-dimensional analysis of blast loaded plates to account for some of these additional loading conditions.



$$\emptyset_c = \frac{I}{\pi R t^2 (\sigma\rho)^{0.5}} \qquad (1)$$

Where R = exposed plate radius, t = plate thickness, I = impulse, $\rho$ = material density, $\sigma$ = characteristic material stress (quasi-static yield stress for monolithic metals) and $\emptyset_c$ is known as the non-dimensional impulse parameter for circular plates.

$$\emptyset_c = \frac{I\left(1+ln\left(R/_{R_o}\right)\right)}{\pi R t^2 (\sigma\rho)^{0.5}} \qquad (2)$$

Where $R_0$ = load radius of a centrally located disc of explosive.

A modification to account for stand-off distance in the response of circular plates was proposed by Jacob et al.[16], shown in Eq. (3), based upon tests conducted over a range of stand-off distances (from 13 to 300 mm) where the blast was directed along a tube towards a 106 mm diameter metal target plate, as described previously.

$$\emptyset_{cs} = \frac{I\left(1+ln\left({}^{R}/_{R_o}\right)\right)}{\left(1+ln\left({}^{S}/_{R_o}\right)\right)\pi R t^2 (\sigma\rho)^{0.5}} \tag{3}$$

Where S = stand off distance (SOD) between charge surface and target plate surface.

Nurick and Martin[2] found an empirical relationship between permanent deflection-thickness ratio and non-dimensional impulse using data from over 100 tests. This relationship, expressing in Eq. (4), is used for large inelastic displacement only, and not for failures involving tensile tearing of the plate (capping in the plate centre or tearing at the boundary) or shear failure (either in the central region or boundary of the plate).

$$\frac{\delta}{t} = 0.425\emptyset_{cs} + 0.277 \tag{4}$$

Where $\delta$ = permanent midpoint deflection of the plate.

The empirical relationship in Eq. (4) was determined from the slope of the non-dimensional displacement versus non-dimensional impulse curve and had a correlation coefficient of 0.974. Since 1990, hundreds of additional tests have been performed on circular plates subjected to various loading conditions. Data from these tests is combined with data obtained prior to 1990 and is plotted in Figure 8 in terms of non-dimensional impulse and non-dimensional displacement. The pre-1990 data went up to a non-dimensional impulse value of approximately 25; 140 of the new data-points are in the range where non-dimensional impulse is between 25 and 50. In total, 699 data-points are plotted in Figure 8, along with a line described by Eq. (4) and a new regression line, given by the expression in Eq. (5). A correlation coefficient of 0.928 is obtained for Eq. (5). As indicated in Table 3, 74% of the data is predicted within a plate thickness and 90% of the data within 2 plate thicknesses of the expression in Eq. (5). There is little difference between the new empirical expression in Eq. (5) and the 1989 proposal[2], validating the original prediction in Eq. (4).

$$\frac{\delta}{t} = 0.427\emptyset_{cs} + 0.298 \qquad (5)$$

From an inspection of Table 3 and Figure 8, it is evident that the additional data agrees particularly well with the data prior to 1990 for non-dimensional impulses below 25. Above a non-dimensional impulse of 25, there is an upward trend in the displacement data away from the lines described by Eqs (4) or (5). At higher non-dimensional impulses, thinning or necking of the plates is likely to be occurring at the boundary, reducing the levels of in-plane restraint and hence increasing the displacement exhibited by those plates as also observed by Nurick and Teeling-Smith[36] for the range of deflection-thickness ratio higher than 10.

It should be noted that the empirical equations presented herein are restricted to mostly mild steel plates which are known to be highly strain rate sensitive. There are a few data points on aluminium plates. The slight variation in the various figures could be related, partly, to the different strain rate sensitive properties of the various mild steels. Jones[37] showed how strain rate effects can be considered for plating under explosive loadings. Yao et al.[38] very recently presented some experimental results on locally blast loaded mild steel plates that were very similar to those presented by Nurick and co-workers[14, 16]. Yao et al. [38] showed that there was a linear trend of increasing displacement-thickness ratio with increasing dimensionless damage number $D_{ex}$, where $D_{ex}$ used the Hopkinson scaled distance (shown in Eq. (6)) instead of impulse (I) as the loading parameter in the dimensionless analysis. This is similar to the approach taken by Yuen et al.[22] for large scale explosions outdoors which employed empirical formulae to estimate the impulse using the peak over-pressure and duration calculations from the Hopkinson scaled distance. However, the stand-off distance range was small (12.9-17.6 mm) and the effects of the charge geometry and plate stiffness were not considered. Hence, this work uses impulse with the appropriate correction factors for stand-off distance, charge shape and plate geometry shown in Eq. (3).

$$Z = \frac{S}{W^{1/3}} \tag{6}$$

Where Z = Hopkinson scaled distance and W = equivalent TNT mass of charge

### 3.2 Quadrangular plates

A similar approach to non-dimensional analysis has been followed for quadrangular plates. The non-dimensional impulse $\phi_q$ (or damage number) for quadrangular plates proposed by Nurick and Martin[2] in 1989 is given in Eq. (7). This was modified by Jacob et al.[14] to incorporate a loading parameter for localised loading, as shown in Eq. (8).

$$\phi_q = \frac{I}{2t^2 \left(BL\rho\sigma\right)^{1/2}} \tag{7}$$

Where B = plate breadth; L = plate length

$$\phi_{ql} = \frac{I\left(1 + \ln\left(\frac{LB}{\pi R_0^2}\right)\right)}{2t^2 (LB\rho\sigma)^{1/2}} \tag{8}$$

In 1989, Nurick and Martin[2] plotted the deflection-thickness ratios obtained from uniform loading tests against the non-dimensional impulse parameter given in Eq. (7). A regression analysis was performed to obtain a line of best fit. The equation of the best fit line was proposed as an empirical prediction for the large deformation response of blast-loaded quadrangular plates and is shown in Eq. (9). A probability of 90% is obtained to predict mid-point deflection within a plate thickness.

$$\left(\frac{\delta}{t}\right)_q = 0.471\,\phi_q + 0.001 \qquad (9)$$

Eq. (8) had a correlation coefficient of 0.984, where the number of data-points was 156. The deflection-thickness ratios of quadrangular plates subjected to uniform and localised loads for all experiments pre-1989 and post-1989 were plotted against the appropriate non-dimensional impulse parameters from Eqs. (7) and (8). The graph is shown in Figure 9 and comprises results from 356 experiments. A new empirical relationship, given by Eq. (10), with a correlation coefficient of 0.94 was obtained from a regression analysis of all 356 data-points.

$$\left(\frac{\delta}{t}\right)_q = 0.506\,\phi_q - 0.158 \qquad (10)$$

A statistical analysis showed that both Eqs. (9) and (10) would predict the mid-point deflection of a quadrangular plate subjected to either localised or uniform blast load with similar probability within one or two plate thickness (72% and 92% respectively), as indicated in Table 4. At higher dimensionless numbers, it appears that Eq. (10) would provide better prediction.

### 3.3 Combining the circular and quadrangular plate data

Nurick and Martin[2] hypothesised that Eqs. (5) and (9) could be used to determine the deflection-thickness ratio of any circular or quadrangular plates subjected to impulsive loading, provided that the plates do not suffer tearing or shear failure. If a circular and quadrangular plate of equal area, thickness and material properties are subjected to impulsive loading over the entire area (that is, uniformly loaded) then the ratio of Eqs. (1) and (7) is:

$$\frac{\phi_c}{\phi_q} = \frac{2}{\pi^{0.5}} = 1.128 \tag{11}$$

If Eq. (11) is substituted into Eq. (5) then a new empirical expression is formulated for plates of either circular or quadrangular geometry, Eq. (12):

$$\frac{\delta}{t} = 0.480\,\phi_q + 0.277 \tag{12}$$

Eq. (11) was used to combine all the experimental data for circular and quadrangular plates, including the locally loaded tests and those performed at various stand-off distances, with the appropriate corrections to $\phi$ given in Eqs. (2), (8) and (3). The deflection-thickness ratios of all plates subjected to blast loads (pre-1989 and post 1989) were plotted against the non-dimensional impulse parameter as shown in Figure 10. A regression analysis was performed and yielded the empirical prediction given by Eq. (13), which has a correlation coefficient of 0.92 for 1054 data-points.

$$\frac{\delta}{t} = 0.446\,\phi_q + 0.261 \tag{13}$$

A statistical analysis, summarised in Table 5, showed that Eq. (13) provides a better correlation for plate prediction than Eq. (12).

## 4. Concluding comments

From the large numbers of experiments conducted since 1989, it has been found that the failure mode progression of circular and quadrangular plates is similar[3, 9]. The Mode I deformation profile of uniformly was characterised by a single global dome, whereas locally loaded plates exhibited a local inner dome atop a global dome profile. Capping and petalling failures occurred in the centre of locally loaded plates, as opposed to tensile and shear failures at the boundaries of uniformly loaded plates[3, 9]. The locally loaded plates have been observed to exhibit tearing at the boundary when the load-plate diameter ratio is increased above 0.4[13]. Boundary conditions have a significant influence on the tearing and shear failures of plates due to the difference in in-plane movement achieved with each boundary condition. Rigid boundaries, such as built-in and welded boundaries, will initiate necking and tearing failures at lower impulses compared to clamped boundaries[5, 10]. The effect of "edge sharpness" of the tensile boundary failure of clamped plates showed that filleting the clamp delayed the onset of tearing by preventing indentation of the plate boundary[6]. Increasing stand-off distance resulted in less localised loading of plates and it was found that when the stand-off distance exceeds the largest plate dimension, loading could be considered to be uniform[16].

The addition of stiffeners reduced the displacements of clamped quadrangular plates subjected to uniformly distributed blast loading, particularly if they were placed along the mid-lines of plates[33]. However, the initiation of tearing along the boundary can occur at lower impulses[33]. In locally loaded stiffened plates, the stiffener placement also affected the tearing location, with tearing initiating along the stiffener-plate edges[15].

In parallel with experimental studies, the non-dimensional analysis used by Nurick and Martin[2] has also been expanded to include the effects of load localisation for quadrangular plates[14] and the influence of stand-off distance for circular plates[16]. When the new post-1989 experimental data is plotted in non-dimensional form, the original empirical predictions proposed in ref[2] are very close to the best fits for the data, with particularly good correlation observed for circular plates. The data for circular and quadrangular plates has been combined into one set and a new empirical prediction is proposed in Eq. (12), which is very similar in form to those previously used. Thus, 25 years on from the original work by Nurick and Martin[2], it is concluded that this analysis technique is still useful and the original empirical predictions give good correlation with experiments. It should be noted that the effects of both strain hardening and strain rate sensitivity have not been specifically considered and that both effects are embedded in the empirical equations.

**Acknowledgements**

The authors wish to thank the staff and students at BISRU for their help, and the Mechanical Engineering workshop at the University of Cape Town for their technical assistance. The authors are grateful to the UCT University Research Committee and the National Research Foundation (NRF) of South Africa for their financial support. Opinions expressed and conclusions arrived at, are those of the authors and are not necessarily to be attributed to the NRF.

**References**

[1] G.N. Nurick, J.B. Martin, Deformation of thin plates subjected to impulsive loading - a review. Part I: Theoretical considerations, International Journal of Impact Engineering, 8 (1989) 159-169.

[2] G.N. Nurick, J.B. Martin, Deformation of thin plates subjected to impulsive loading - a review. Part II: Experimental Studies, International Journal of Impact Engineering, 8 (1989) 171-186.

[3] R.G. Teeling-Smith, G.N. Nurick, The deformation and tearing of thin circular plates subjected to impulsive loads, International Journal of Impact Engineering, 11 (1991) 77-91.

[4] S.B. Menkes, H.J. Opat, Tearing and shear failures in explosively loaded clamped beams, Experimental Mechanics, 13 (1973) 480-486.

[5] B.M. Thomas, G.N. Nurick, The effect of boundary conditions on thin plates subjected to impulsive loads, The 5th International Symposium on Plasticity and its Current Application, (1995) 85-88.

[6] G.N. Nurick, M.E. Gelman, N.S. Marshall, Tearing of blast loaded plates with clamped boundary conditions, International Journal of Impact Engineering, 18 (1996) 803-827.

[7] T.J. Cloete, G.N. Nurick, R.N. Palmer, The deformation and shear failure of peripherally clamped centrally supported blast loaded circular plates, International Journal of Impact Engineering, 32 (2005) 92-117.

[8] M.D. Olson, J.R. Fagnan, G.N. Nurick, Deformation and rupture of blast loaded square plates - Predictions and experiments, International Journal of Impact Engineering, 12 (1993) 279-291.

[9] G.N. Nurick, G.C. Shave, The deformation and tearing of thin square plates subjected to impulsive loads-an experimental study, International Journal of Impact Engineering, 18 (1996) 99-116.

[10] D. Bonorchis, G.N. Nurick, The effect of welded boundaries on the response of rectangular hot-rolled mild steel plates subjected to localised blast loading, International Journal of Impact Engineering, 34 (2007) 1729-1738.

[11] T. Wierzbicki, G.N. Nurick, Large deformation of thin plates under localised impulsive loading, International Journal of Impact Engineering, 18 (1996) 899-918.

[12] G.N. Nurick, A.M. Radford, Deformation and tearing of clamped circular plates subjected to localised central blast loads, Recent developments in computational and applied mechanics: a volume in honour of John B. Martin, (1997) 276-301.

[13] S. Chung Kim Yuen, G.N. Nurick, The significance of the thickness of a plate when subjected to localised blast load, 16th International Symposium on Military Aspects of Blast and Shock, (MABS 16), (2000) 491-499.

[14] N. Jacob, S. Chung Kim Yuen, G.N. Nurick, D. Bonorchis, S.A. Desai, D. Tait, Scaling aspects of quadrangular plates subjected to localised blast loads - experiments and predictions, International Journal of Impact Engineering, 30 (2004) 1179-1208.

[15] G.S. Langdon, S. Chung Kim Yuen, G.N. Nurick, Experimental and numerical studies on the response of quadrangular stiffened plates -Part II- subjected to localised load, International Journal of Impact Engineering, 31 (2005) 85-111.

[16] N. Jacob, G.N. Nurick, G.S. Langdon, The effect of stand-off distance on the failure of fully clamped circular mild steel plates subjected to blast loads, Engineering Structures, 29 (2007) 2723-2736.

[17] A. Neuberger, S. Peles, D. Rittel, Scaling the response of circular plates subjected to large and close-range spherical explosions. Part I: Air-blast loading, International Journal of Impact Engineering, 34 (2007) 859-873.

[18] A. Neuberger, S. Peles, D. Rittel, Springback of circular clamped armor steel plates subjected to spherical air-blast loading, International Journal of Impact Engineering, 36 (2009) 53-60.

[19] A.C. Jacinto, R.D. Ambrosini, R.F. Danesi, Experimental and computational analysis of plates under air blast loading, International Journal of Impact Engineering, 25 (2001) 927-947.

[20] D. Bonorchis, G.N. Nurick, The influence of boundary conditions on the loading of rectangular plates subjected to localised blast loading - Importance in numerical simulations, International Journal of Impact Engineering, 36 (2009) 40-52.
[21] G.N. Nurick, S. Chung Kim Yuen, N. Jacob, W. Verster, D. Bwalya, A.R. Vara, Response of Quadrangular Mild-Steel Plates to Large Explosive Load, 2nd International Conference on Design and Analysis of Protective Structures (DAPS), (2006) 30-44.
[22] S. Chung Kim Yuen, G.N. Nurick, W. Verster, N. Jacob, A.R. Vara, V.H. Balden, D. Bwalya, R.A. Govender, M. Pittermann, Deformation of mild steel plates subjected to large-scale explosions, International Journal of Impact Engineering, 35 (2008) 684-703.
[23] R. Houlston, J.E. Slater, N. Pegg, C.G. DesRochers, On analysis of structural response of ship panels subject to air blast loading, Computers and Structures, 21 (1985) 273-289.
[24] R. Houlston, C.G. DesRochers, Nonlinear structural response of ship panels subjected to air blast loading, Computers and Structures, 26 (1987) 1-15.
[25] R.B. Schubak, M.D. Olson, D.L. Anderson, Nonlinear analysis of one-way stiffened plates under blast loads, Structures Under Shock and Impact I, (SUSI I), (1989) 345-354.
[26] R.B. Schubak, M.D. Olson, D.L. Anderson, Non-linear rigid-plastic analysis of stiffened plates under blast loads, in: P.S. Bulson (Ed.) Structures Under Shock and Impact II, (SUSI II), Computational Mechanics Publications, Portsmouth, UK, 1992, pp. 521-532.
[27] R.B. Schubak, M.D. Olson, D.L. Anderson, Rigid-plastic modelling of blast loaded stiffened plates - Part I: one way stiffened plates, Third International Symposium on Structural Crashworthiness and Failure, (1993).
[28] R.B. Schubak, M.D. Olson, D.L. Anderson, Rigid-plastic modelling of blast loaded stiffened plates - Part II: partial end fixity, rate effects and two-way stiffened plates, Third International Symposium on Structural Crashworthiness and Failure, (1993).
[29] G.N. Nurick, A.G. Conolly, Response of clamped single and double stiffened rectangular plates subjected to blast loads, Structures Under Shock and Impact III (SUSI III), (1994) 207-220.
[30] G.N. Nurick, M.D. Olson, J.R. Fagnan, A. Levin, Deformation and tearing of blast-loaded stiffened square plates, International Journal of Impact Engineering, 16 (1995) 273-291.
[31] G.N. Nurick, D.M. Lumpp, Deflection and tearing of clamped stiffened circular plates subjected to uniform impulsive blast loads, Structures Under Shock and Impact IV (SUSI IV), (1996) 393-402.
[32] G.K. Schleyer, S.S. Hsu, M.D. White, R.S. Birch, Pulse pressure loading of clamped mild steel plates, International Journal of Impact Engineering, 28 (2003) 223-274.
[33] S. Chung Kim Yuen, G.N. Nurick, Experimental and numerical studies on the response of quadrangular stiffened plates -Part I- subjected to uniform blast load, International Journal of Impact Engineering, 31 (2005) 55-83.
[34] R.L. Veldman, J. Ari-Gur, C. Clum, A. DeYoung, J. Folkert, Effects of pre-pressurization on blast response of clamped aluminum plates, International Journal of Impact Engineering, 32 (2006) 1678-1695.
[35] R.L. Veldman, J. Ari-Gur, C. Clum, Response of pre-pressurized reinforced plates under blast loading, International Journal of Impact Engineering, 35 (2008) 240-250.
[36] G.N. Nurick, R.G. Teeling-Smith, Predicting the onset of necking and hence tearing of thin plates subjected to impulsive loads - an experimental view, Structures Under Shock and Impact II (SUSI II), (1994) 431-445.

[37] N. Jones, Dynamic inelastic response of strain rate sensitive ductile plates due to large impact, dynamic pressure and explosive loadings, International Journal of Impact Engineering, 74 (2014) 3-15.
[38] S. Yao, D. Zhang, F. Lu, Dimensionless numbers for dynamic response analysis of clamped square plates subjected to blast loading, Archive of Applied Mechanics, 85 (2015) 735-744.

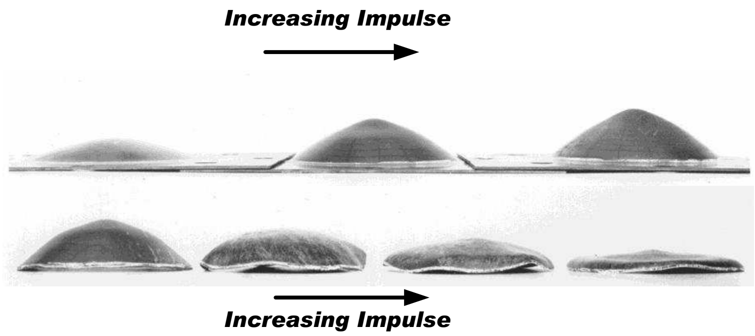


Figure 1: Photographs showing the failure of uniformly loaded circular plates with increasing impulse [3]

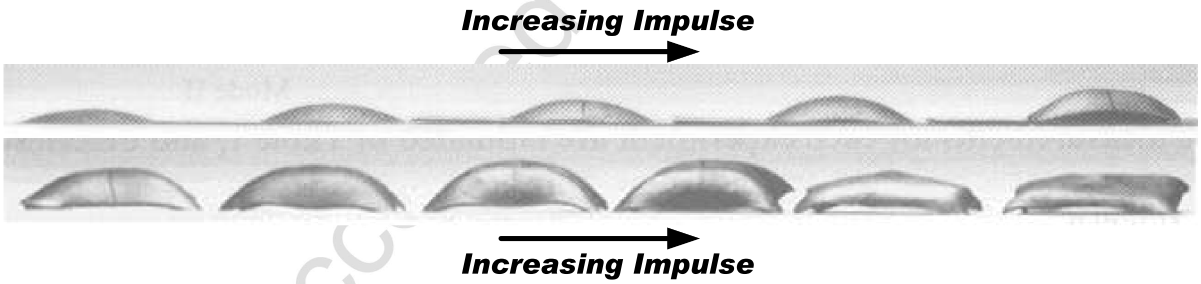


Figure 2: Photographs showing the failure of uniformly loaded square plates with increasing impulse [9]

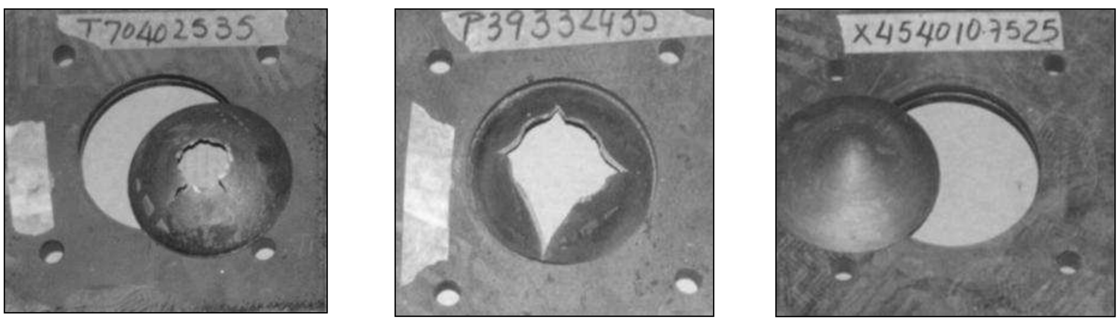

(a) Capping failure (b) Petalling failure (c) Tensile tearing at the boundary

Figure 3: Photographs of locally loaded circular plates [13]

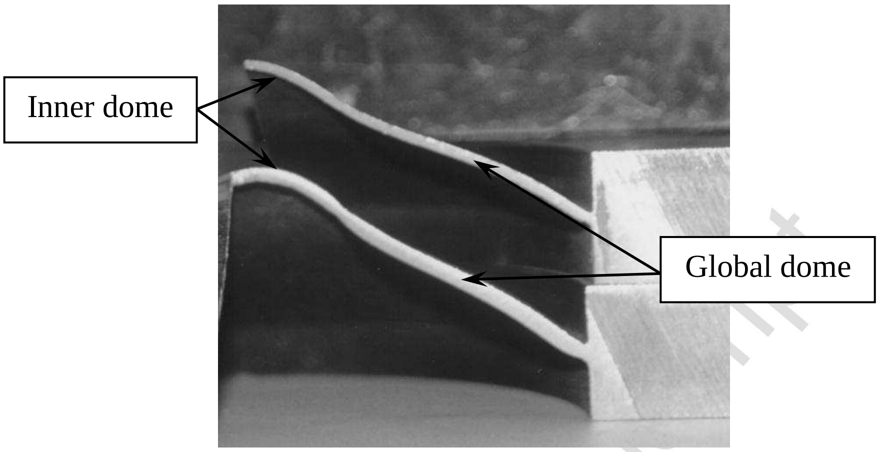


Figure 4: Photographs of cross-sections from two built-in circular plates subjected to localised blast loading [13]

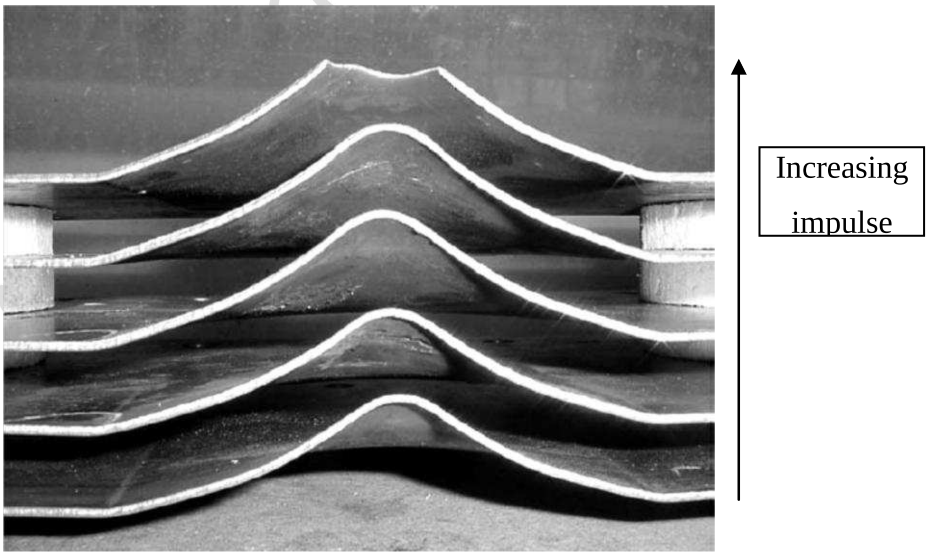


Figure 5: Photographs of cross-sectional profiles from quadrangular plates subjected to localised blast loading [14]

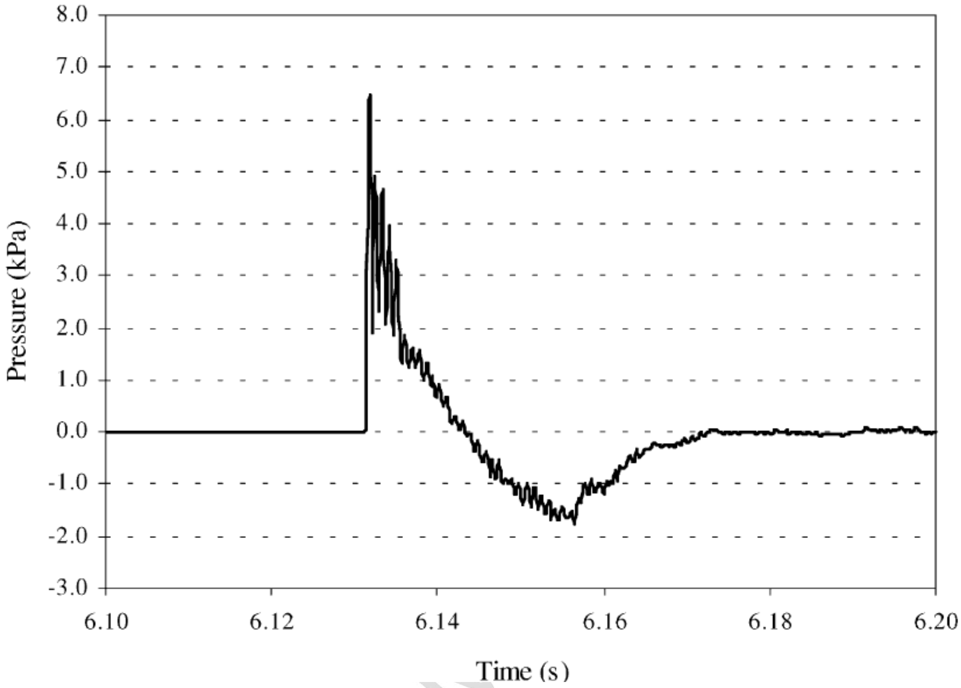


Figure 6: Pressure-time history recorded from a far-field explosion, Jacinto et al. [19]

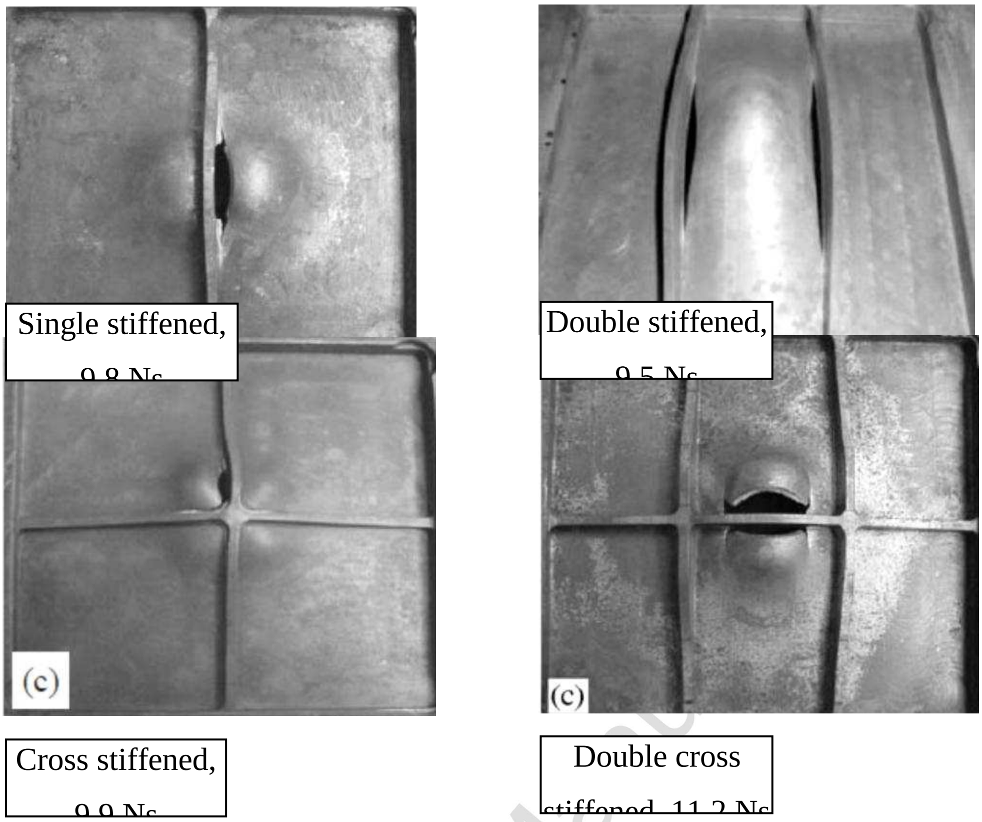


Figure 7: Photographs showing the tearing locations of various stiffened plates subjected to localised blast loading [15]

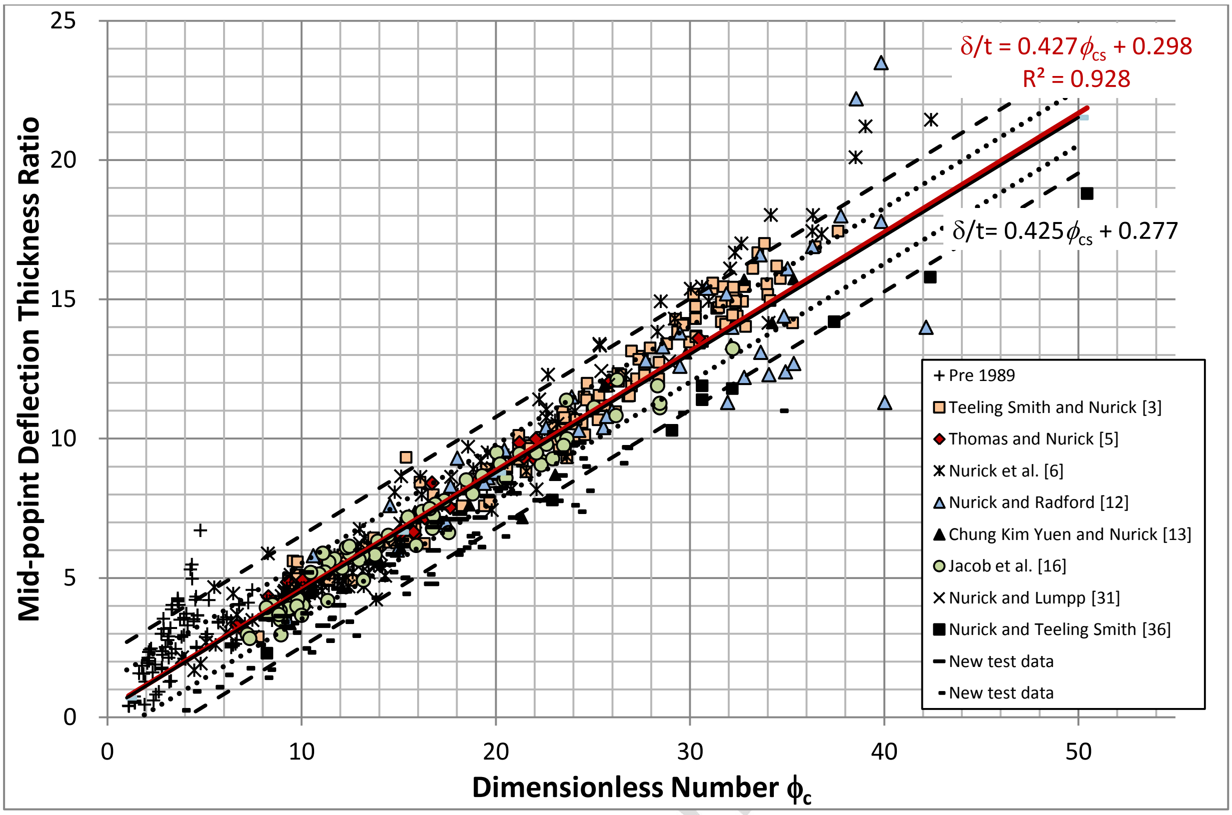


Figure 8: Graph of displacement-thickness ratio versus non-dimensional impulse for circular plates, both pre-1989 and post-1989

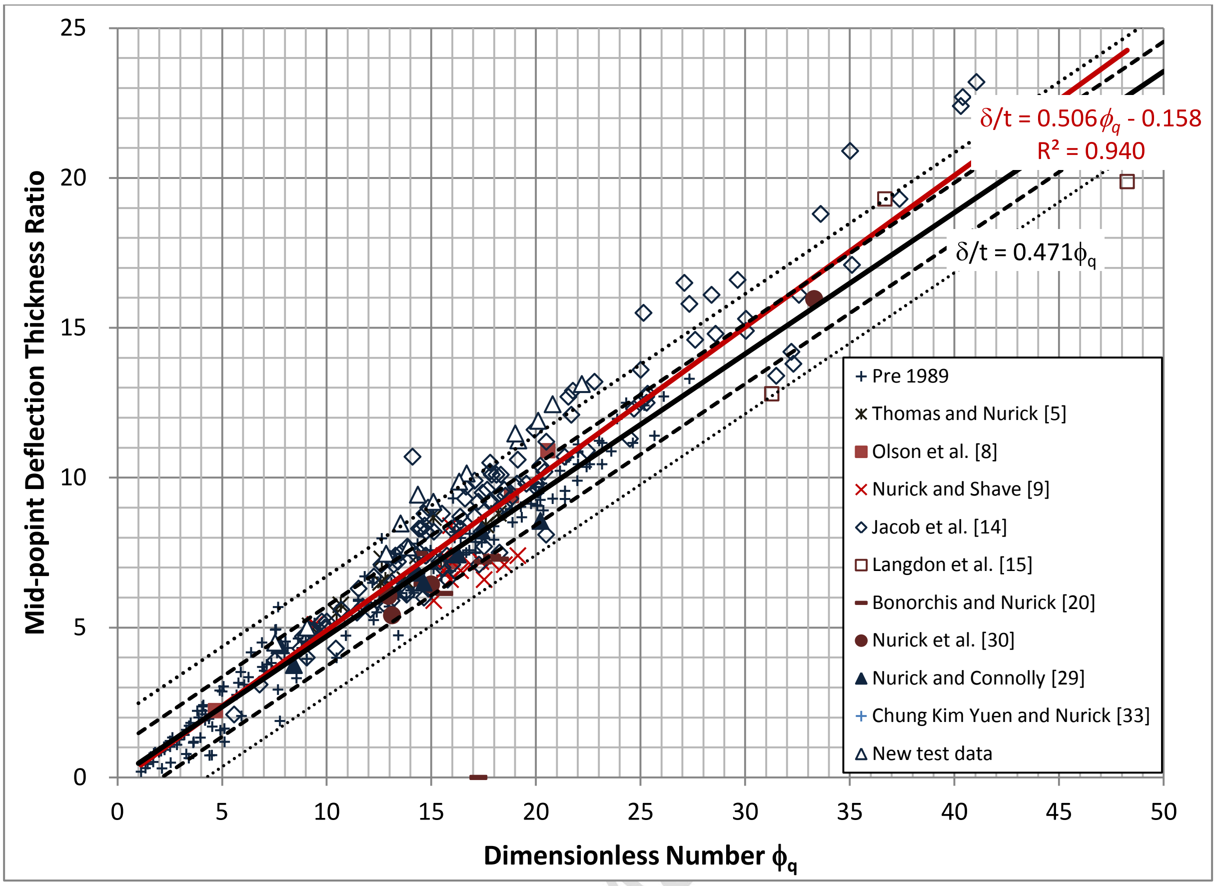




Figure 9: Graph of displacement-thickness ratio versus non-dimensional impulse for quadrangular plates, both pre-1989 and post-1989

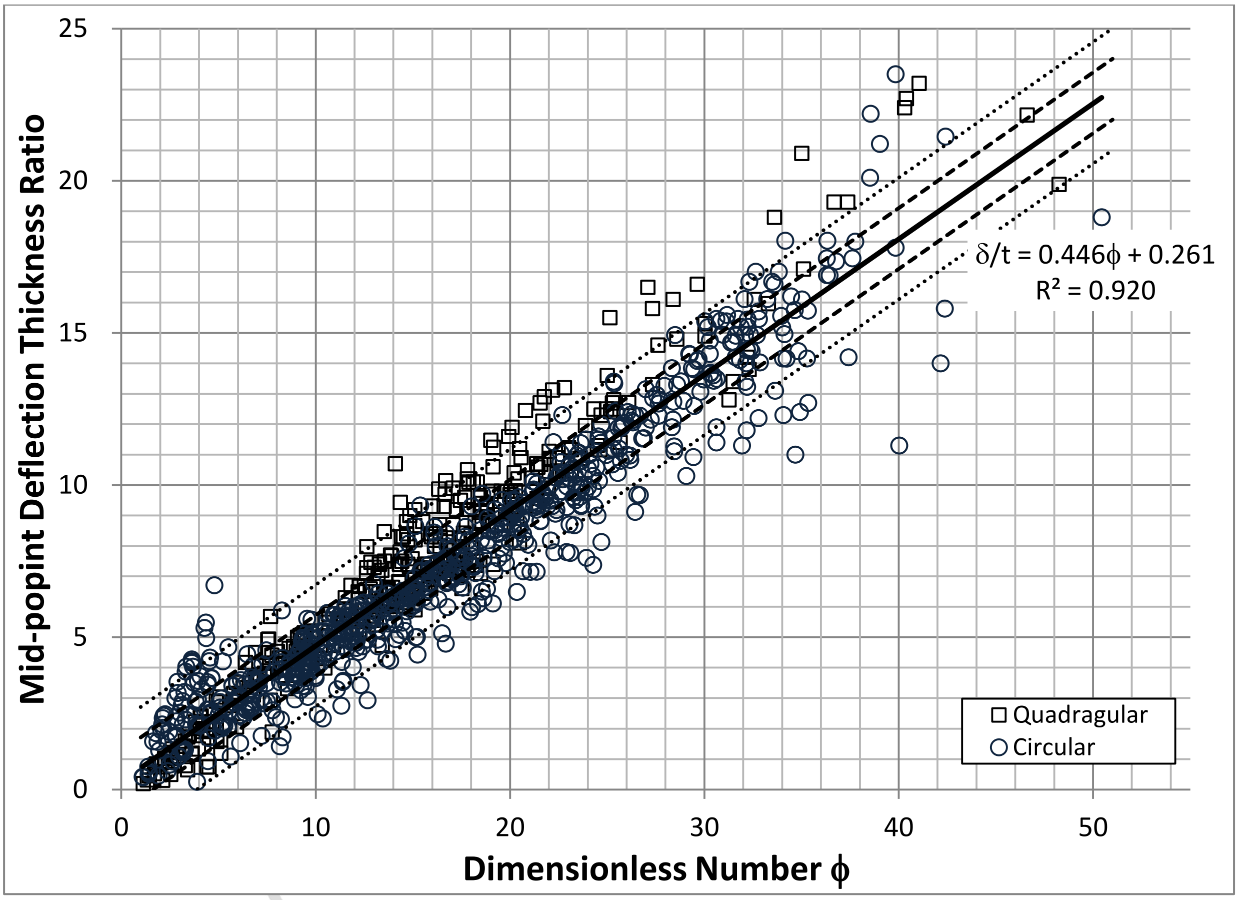


Figure 10: Graph of displacement-thickness ratio versus non-dimensional impulse for the combined circular and quadrangular plate data, both pre-1989 and post-1989

680 Table 1: Summary of experiments performed since 1989 on air-blast loaded metal plates

| Load type | Plate type[1] | Reference | Notes | Nominal Plate dimensions (mm) | Year |
|---|---|---|---|---|---|
| Uniform | C | Teeling-Smith and Nurick [3] | Failure Modes I, II and III of circular plates | ∅ 500 - 1000 x 10 - 20 | 1991 |
| | | Thomas and Nurick [5] | Built-in versus clamped boundaries | ∅ 100 x 1.6 | 1995 |
| | | Nurick et al [6] | Influence of edge sharpness: clamped plates | ∅ 60 -120 x 1.6 | 1996 |
| | | Cloete et al [7] | Annular and centrally support plates, failure | ∅ 100 x 1.6 | 2005 |
| | Q | Olson et al [8] | Failure progression, tearing initiation | 89 x 89 x 1.6 | 1993 |
| | | Nurick and Shave [9] | Failure progression, tearing initiation | 89 x 89 x 1.6 | 1996 |
| | | Bonorchis and Nurick [10] | Varied boundary conditions | 188 – 200 x 108 - 120 x 3 | 2007 |
| Localised | C | Wierzbicki and Nurick [11] | Failure modes | ∅ 100 x 1.6 | 1996 |
| | | Nurick and Radford [12] | Failure modes, capping | ∅ 100 x 1.6 | 1997 |
| | | Yuen and Nurick [13] | Influence of plate thickness, load-to-plate diameter ratio | ∅ 100 x 1.6 - 3.6 | 2000 |
| | Q | Jacob et al. [14] | Varied load and plate geometries | 160 – 290 x 160 - 290 x 1.6 – 4.0 (different aspect ratios) | 2004 |
| | | Langdon et al. [15] | Flat and stiffened plates | 126 x 126 x 1.6 | 2005 |
| Stand-off distance | C | Jacob et al. [16] | Influence of stand-off distance on Mode I failure, use of tube to direct blast | ∅ 106 x 1.9 | 2007 |
| | | Yao et al. [38] | Mild steel, 12.9 – 17.6 mm stand-off distance, dimensionless analysis | 160 x 160 x 1.6 -4.0 | 2015 |
| | | Neuberger et al. | Scaling | ∅ 100 x 1.6 | 2007 |

| | | | | | |
|---|---|---|---|---|---|
| | | [17] | | | |
| | | Neuberger et al. [18] | Springback of armour steel | ∅ 1000 x 20 | 2009 |
| | Q | Jacinto et al. [19] | Boundary conditions, model validation | 950 – 1000 x 950 – 1500 x 0.9 – 2.1 | 2001 |
| | | Yuen et al. [21, 22] | Large scale field tests, scaling | 500 x 500 x 3-6 | 2006 |
| Uniform | QS | Schubak et al [25-28] | One and two way stiffeners, model validation | 4000 - 4572 x 2438 – 4000 x 6 - 7 | 1992-1993 |
| | | Nurick et al.[30] | Influence of integral stiffeners | 89 x 89 x 1.6 | 1995 |
| | | Schleyer et al[32] | Effects of loading direction, in-plane restraint on pulse loaded welded stiffened plates | 1000 x 1000 x 2 | 2003 |
| | | Yuen and Nurick [33] | Influence of integral stiffeners | 126 x 126 x 1.6 | 2005 |
| | | Veldman [34] | Riveted stiffened plates, pre-pressurisation | 508 x 610 x 1.6 | 2008 |

[1]C = circular, Q = quadrangular, QS = quadrangular stiffened

[1]C = circular, Q = quadrangular, QS = quadrangular stiffened

Table 2: Descriptions of failure modes for plates subjected to uniformly and locally distributed blast loading, according to Jacob et al [16]

| **Failure Mode** | **Description** | **Uniform loading** | **Localised loading** |
|---|---|---|---|
| Mode I | large inelastic deformation | ✓ | ✓ |
| Mode Ia | large inelastic deformation with necking around part of the boundary | ✓ | |
| Mode Ib | large inelastic deformation with necking around the entire boundary | ✓ | ✓ |
| Mode Itc | large inelastic deformation with thinning in the central area | | ✓ |
| Mode II* | large inelastic deformation with partial tearing around part of the boundary | ✓ | |
| Mode II*c | partial tearing in the central area | | ✓ |
| Mode II | tensile tearing at the boundary | ✓ | ✓ |
| Mode IIa | increasing mid-point deflection with increasing impulse with complete tearing at the boundary | ✓ | |
| Mode IIb | decreasing mid-point deflection with increasing impulse with complete tearing at the boundary | ✓ | |
| Mode IIc | complete tearing in the central area – capping | | ✓ |
| Mode III | transverse shear failure at the boundary | ✓ | |
| Petalling | | | ✓ |

Table 3: Statistical variation of deflection-thickness ratio for circular plates subjected to blast load for all data

| | Number of data points | ±1 plate thickness | ±2 plate thickness |
|---|---|---|---|
| $\phi_c$ , Eq. (4) | 699 | 74% | 90% |
| $0 \leq \phi_c \leq 25$ | 559 | 80% | 93% |
| $\phi_c > 25$ | 140 | 49% | 77% |

Table 4: Statistical variation of deflection-thickness ratio for quadrangular plates subjected to blast load for all data

| | Number of data points | ±1 plate thickness | ±2 plate thickness |
|---|---|---|---|
| $\phi_q$ , Eq.(8) | 354 | 72% | 94% |
| $0 \leq \phi_q \leq 25$ | 320 | 77% | 96% |
| $\phi_q > 25$ | 34 | 47% | 65% |
| $\phi_q$ , Eq.(9) | 354 | 73% | 92% |
| $0 \leq \phi_q \leq 25$ | 320 | 74% | 97% |
| $\phi_q > 25$ | 34 | 44% | 65% |

Table 5: Statistical variation of deflection-thickness ratio for the combined circular and quadrangular plate data

| | ±1 plate thickness | ±2 plate thickness |
|---|---|---|
| Eq. (12) | 61% | 88% |
| Eq. (13) | 71% | 89% |